

Microfluidic Platform for Adherent Single Cell High-Throughput Screening

Paola OCCHETTA¹, Chiara MALLOGGI², Andrea GAZANEO¹, Mara LICINI¹, Alberto REDAELLI¹,
Gabriele CANDIANI², Marco RASPONI^{1*}

* Corresponding author: Tel.: +39 (02) 2399 3377; Email: marco.rasponi@polimi.it

¹ Department of Electronics, Information and Bioengineering, Politecnico di Milano, Milano, Italy

² Department of Chemistry, Materials and Chemical Engineering "Giulio Natta", Politecnico di Milano, Milano, Italy

Abstract Traditionally, *in vitro* investigations on biology and physiology of cells rely on averaging the responses eliciting from heterogeneous cell populations, thus being unsuitable for assessing individual cell behaviors in response to external stimulations. In the last years, great interest has thus been focused on single cell analysis and screening, which represents a promising tool aiming at pursuing the direct and deterministic control over cause-effect relationships guiding cell behavior. In this regard, a high-throughput microfluidic platform for trapping and culturing adherent single cells was presented. A single cell trapping mechanism was implemented based on dynamic variation of fluidic resistances. A round-shaped culture chamber ($\Phi=250\mu\text{m}$, $h=25\mu\text{m}$) was conceived presenting two connections with a main fluidic path: (i) an upper wide opening, and (ii) a bottom trapping junction which modulates the hydraulic resistance. Several layouts of the chamber were designed and computationally validated for the optimization of the single cell trapping efficacy. The optimized chamber layouts were integrated in a polydimethylsiloxane (PDMS) microfluidic platform presenting two main functionalities: (i) 288 chambers for trapping single cells, and (ii) a chaotic-mixer based serial dilution generator for delivering both soluble factors and non-diffusive molecules under spatio-temporally controlled chemical patterns. The devices were experimentally validated and allowed for trapping individual U87-MG (human glioblastoma-astrocytoma epithelial-like) cells and culturing them up to 3 days.

Keywords: Microfluidics, Single Cell, High-Throughput Screening, Chaotic Mixing, Gene Delivery

1. Introduction

Traditionally, *in vitro* investigations on biology and physiology of cells rely on averaging the responses eliciting from heterogeneous cell populations. This approach provides a collective information derived from the integration of multiple, time-variable signals, thus being unsuitable for assessing individual cell evolution as a consequence of external stimulation (Schmid et al., 2010). In the last years, great interest has been focused on single cell analysis and screening, which represents a promising tool aiming at pursuing the direct and deterministic control over cause-effect relationships guiding cell behavior (Lindström and Andersson-Svahn, 2011). However, the analysis on single cells still

presents a variety of challenges. First, in order to obtain a meaningful on cellular heterogeneity, the ability to handle a large number of individual cells in a high-throughput fashion is crucial (Wang, 2012). Moreover, the capability of reliably allocate individual cells in well-defined spatial positions is fundamental for subsequent analyses, often implying the tracking of cells over the culture time (Hong et al., 2012). Finally, the typical size of single-cells demands more strict requirements with respect to standard culture tools, in terms of sensitivity, selectivity and temporal resolution (Love et al., 2013).

Recent advances in microtechnologies and microfabrication are offering increasing cues for addressing these challenges. First, the

reduction of scale leads to unique fluidic phenomena combined with higher surface-to-volume ratios, thus resulting in short reaction times, high reaction efficiencies, and low material consumption (El-Ali et al., 2006). Moreover, the ability of microfluidics to manipulate fluid flows and particles within micrometer-sized channels allows for cells handling to precise spatial configurations and high-throughput analyses under time- and space-controlled conditions (Mu et al., 2013). In the last few years, several strategies have been proposed for single cell manipulations within microfluidic devices, being successfully exploited in several fields of cell biology (Andersson and van den Berg, 2003). The existing approaches for trapping single cells though mainly require complex and expensive fabrication procedures due either to the necessity of multi-layered devices (Hanke et al., 2012; Lawrenz et al., 2012; Wheeler et al., 2003) or to the requirement for feature having sizes difficult to achieve in a reproducible manner through conventional photolithographic techniques (Hong et al., 2012). Herein, a low cost and single-layer PDMS microfluidic platform is presented for isolation and culture of a large number of individual adherent cells into defined spatial configurations. The platform represents a powerful and versatile tool for high-throughput screening on single cells, integrating a serial dilution generator, based on resistive flow, which allows for delivering both soluble factors and non-diffusive molecules under spatio-temporally controlled chemical patterns.

2. Materials and methods

2.1 Design of the Single cell trapping chamber

A microfluidic unit layout was designed aiming at trapping single adherent cells while ensuring enough space for their subsequent culture and proliferation (Fig. 1a-b). In detail, a round-shaped culture chamber ($\Phi=250\mu\text{m}$, $h=25\mu\text{m}$) was conceived presenting two connections with a main fluidic path: (i) an upper (upstream) wide opening which allows

for both transportation of cells and diffusion of media/conditioning factors, and (ii) a bottom (downstream) trapping junction which modulates the hydraulic resistance (Fig. 1a). The mechanism of trapping exploits an automatic variation of hydraulic resistance within the chamber, as schematically depicted in Fig. 1b. Briefly, a cell entering the chamber follows the flow stream, eventually reaching the trapping junction (blue trajectory); the subsequent partial, or total, occlusion of the trap through the cell body causes an increase in terms of hydraulic resistance, and, in turn, a reduction of inflow into the chamber, thus inhibiting the entrance of further cells (red trajectory).

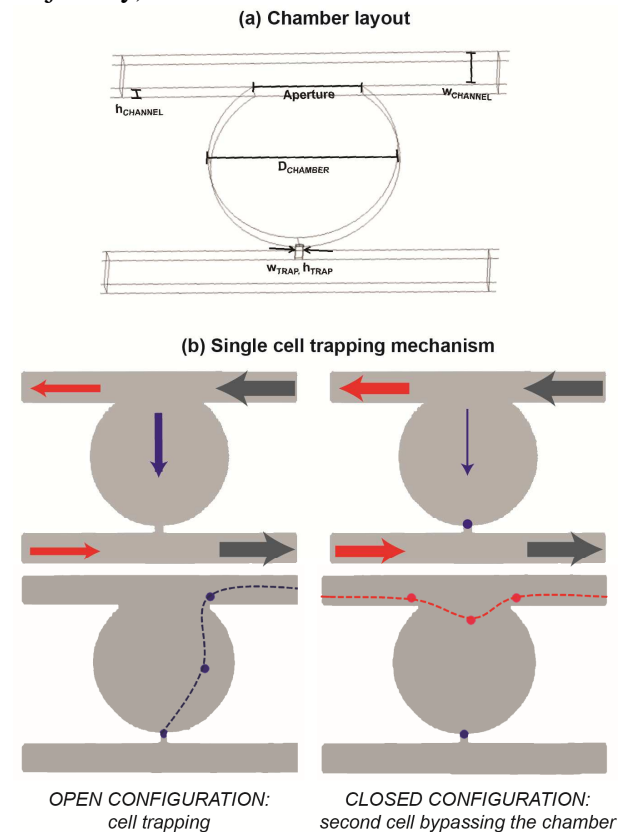


Fig. 1. Round-shaped culture chamber layout for single cell trapping. The chamber ($\Phi=250\mu\text{m}$, $h=25\mu\text{m}$) presents two connections with the main channel: an upstream aperture and a downstream smaller trapping junction (a). The mechanism of trapping exploits an automatic variation of hydraulic resistance within the chamber (b).

The geometry of the chamber was optimized for single cell trapping by means of Computational Fluid Dynamic models (CFD, Comsol Multiphysics).

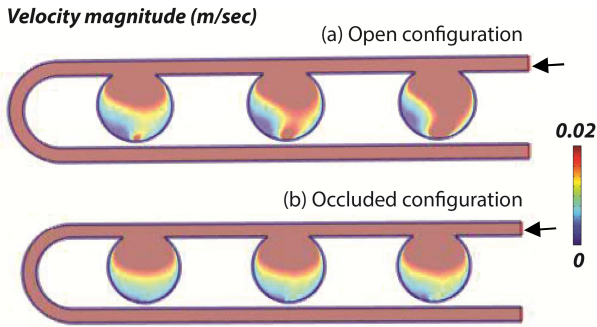


Fig. 2. CFD simulations showing the flow rate partition within a fluidic trapping unit in (a) open and (b) occluded configurations. Shown results were obtained for $Q=0.2 \mu\text{l}/\text{min}$.

For ease of microfabrication, the heights of both fluidic (consisting of flow channels and culture chambers) and trapping layers were fixed at $25\mu\text{m}$ and $5\mu\text{m}$, respectively. Finite element analyses were performed on a 3D model of a fluidic unit (Fig.2), constituted by three culture chambers (provided with trapping elements), and a curved main channel (upstream and downstream). Eight geometries were considered, as combinations of four different widths of the fluidic channels ($25, 50, 75$ and $100\mu\text{m}$) and two widths of the trapping elements (10 and $15\mu\text{m}$). Furthermore, each configuration was characterized by either the absence or presence of trapped cells. Trapped cells were modeled as solid spheres (diameter either of 10 or $16\mu\text{m}$), slightly intersecting the boundaries in proximity of the trapping element, and thus partially occluding the trap junction. The distribution of the inflow among each chamber was assessed and compared for all configurations (Fig.2). The geometries were discretized through a tetrahedral mesh, consisting of about 250×10^3 elements. The flow field was computed by solving stationary Navier–Stokes equations for incompressible fluids, setting the density and the viscosity equal to those of water at 25°C ($1000 \text{ kg}/\text{m}^3$ and 0.890 cP , respectively). A uniform velocity profile was applied to the inlet, corresponding to a total inflow of $0.2\mu\text{l}/\text{min}$, while a constant pressure condition was set to the outlet. No-slip conditions were applied to boundary walls. Convergence criterion was set as when residuals were reduced by four orders of magnitude. For each channel width, the minimum inflow required to guarantee the

entrance of at least one cell into the chamber was numerically estimated (Q_{lim}) and compared with the results of the partition of the flow for the different layouts. By assuming cells move along the streamlines passing through their centers, Q_{lim} is the maximum flow rate which allows the entrance of portion of fluid into the chambers having width equal to the radius of a cell. These calculations were carried out considering two different cell sizes ($\Phi = 10$ and $16\mu\text{m}$), thus yielding two different Q_{lim} . A selectivity index (SI) was then defined for comparing the 8 chamber layouts in terms of single cell trapping ability. SI was calculated as percentage difference between Q_{lim} and flow rate in closed configuration (Q_c):

$$SI = 100 * \left(\frac{Q_{\text{lim}} - Q_c}{Q_{\text{lim}}} \right)$$

2.2 Design of the chaotic mixer serial dilution generator

A chaotic mixer serial dilution generator (SDG) was integrated within the microfluidic platform for mixing both soluble factors and non-diffusive molecules, splitting an initial concentrated solution into 6 linear dilutions (from 0% to 100% in steps of 20%). The chaotic mixer SDG was designed based on a resistive flow model consisting of symmetric microfluidic networks (Jeon et al., 2000) composed of thin fluidic-resistance microchannels ($60\mu\text{m}$ wide and $25\mu\text{m}$ tall) whose lengths were dimensioned to allow diffusive mixing of soluble factors. Furthermore, aiming at mixing non-diffusive molecules, staggered herringbone (HB) grooves were integrated on the top of the channels (Stroock et al., 2002). Each HB was designed $24\mu\text{m}$ wide and $9\mu\text{m}$ high, being an HB unit constituted of eight HBs changing their orientation between half cycles. The mixing efficiency was computed through finite element analysis by means of Computational Fluid Dynamic models (CFD, Comsol Multiphysics). Finite element analyses were performed on 3D T-shaped HB grooved channel varying the number of repeated HB

units (each $416\mu\text{m}$ long), and using rectangular channels as controls. The geometries were discretized through a tetrahedral mesh, being each unit discretized with about 195×10^3 and 20×10^3 elements, in the case of presence and absence of HB respectively. The flow field was computed by solving stationary Navier–Stokes equations as described above, while the mass balance equation were solved to describe the transport of the diluted species. Uniform velocity profiles were applied to the inlets, corresponding to Reynolds numbers (Re) comprised between 0.1 and 10 ($Q=0.255\text{--}25.5\mu\text{l}/\text{min}$), while a constant pressure condition was set to the outlet. A non-diffusive species was injected at a constant concentration in only one inlet and the concentration distribution at 10 equally distributed cross-sections was computed. Fig. 3 shows the trend of species concentrations for $Re=0.1$, demonstrating the achievement of a complete mixing between the two species in a HB grooved channels consisting in the repetition of ten HBs units (total length= 4.2mm), (Fig. 3a), while no mixing was observed in a rectangular channel featuring the same total length (Fig. 3b). The induced chaotic flow was thus demonstrating to enhance the mixing of non-diffusive species, thus decreasing length of the generator itself, which finally occupied a footprint of about 2.5cm^2 .

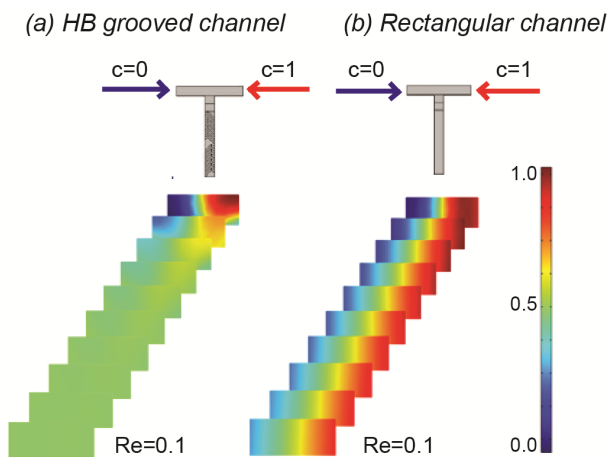


Fig. 3. CFD simulations were computed to verify the mixing efficacy of staggered herringbone (HB) grooves (a) in comparison with rectangular channels (b). Shown results were obtained for $Re=0.1$.

2.3 Fabrication of the microfluidic platform

The final chip layouts were designed integrating the computationally optimized versions of both the trapping chamber and the HBs mixing unit. In detail, the final microfluidic platforms featured an upstream chaotic mixer serial dilution generator, which independently delivered six linear dilutions of an inflow concentrated solution to six downstream culture units. Each culture unit consisted in the repetition of 48 single cell trapping chambers and was integrated with a lateral seeding channel. Two secondary inlets were finally included in the layouts to facilitate the medium change operations, defining a by-pass for the device.

The described layouts were designed through CAD software (AutoCAD, Autodesk Inc.) and corresponding master molds were realized through standard photolithography techniques (Xia and Whitesides, 1998). In particular, three layers were integrated: (i) a rectangular $25\mu\text{m}$ thick layer constituting both fluidic channels and chambers; (ii) a rectangular $9\mu\text{m}$ thick layer for the HB structures, positioned on the top of the previous one, and (iii) a $5\mu\text{m}$ thick layer for the trapping junctions, rendered round shaped after the fabrication re-flow process.

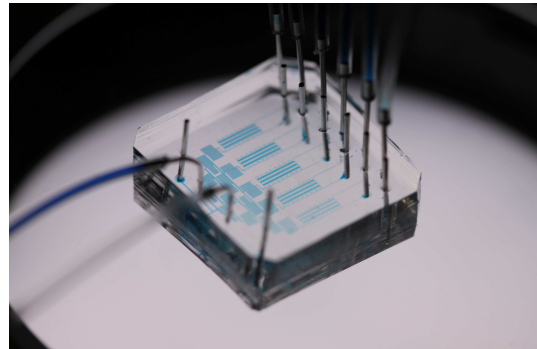
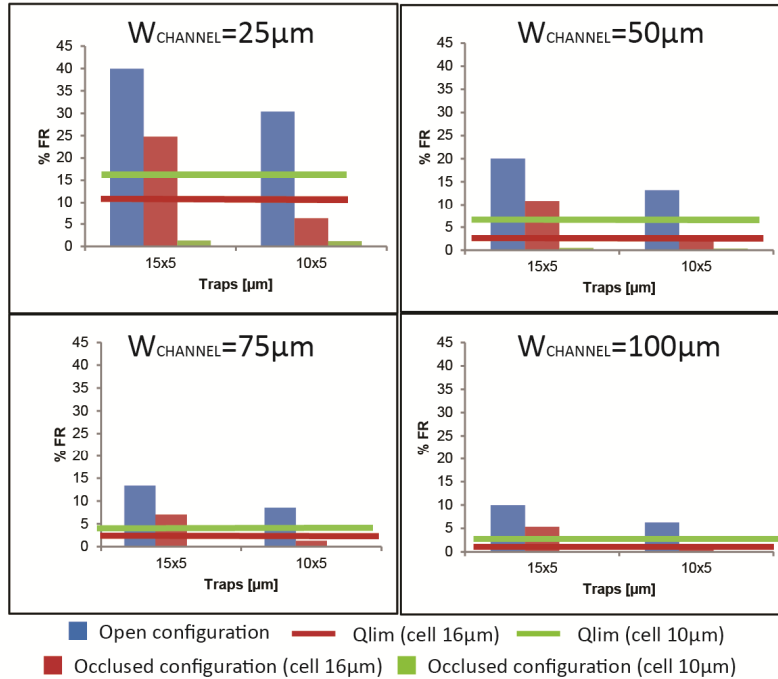


Fig. 4. Microfluidic device

The microfluidic chips (Fig. 4) were then obtained by replica molding of PDMS (Sylgard[®] Dow Corning) on the master mold. Briefly, PDMS was cast on the mold in ratio 10:1 w/w (pre-polymer to curing agent), degassed and cured at 80°C for 3 h. Input and output ports were obtained through a 0.5mm biopsy puncher (Harris Uni-Core[™]) and the PDMS chip was finally permanently bonded to a glass slide ($25 \times 75 \times 1\text{mm}$;) upon a 1 min of air plasma treatment (Harrick Plasma).

(a) - Flow rate partition



(b) - Trapping selectivity index (SI)

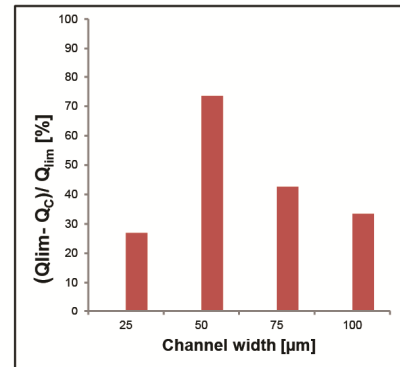


Fig. 5. Distribution of the flow rate inside chamber in open and closed configurations (for both 10 μ m and 16 μ m trapped cells) for the eight considered layouts. The results were then compared with Qlim (a) Trapping selectivity index trend for the layouts featuring 10 μ m wide traps considering trapped cells with a diameter of 10 μ m (b).

2.4 Cell cultures

U87-MG (human glioblastoma-astrocytoma epithelial-like) cell line was purchased from the American Type Culture Collection (ATCC, Manassas, VA, USA). Cells were cultured at 37°C in a humidified atmosphere containing 5% CO₂ in Dulbecco's Modified Eagle Medium (DMEM, Sigma-Aldrich, Milano, Italy) supplemented with 1mM sodium pyruvate, 10mM HEPES buffer, 100U/mL penicillin, 0.1mg/mL streptomycin, 2mM glutamine, and 10% (v/v) fetal bovine serum (FBS) (referred as to complete DMEM).

2.5 Single cell trapping and culturing within the microfluidic device

Preliminary biological experiments were conducted on the computationally optimized platforms to evaluate the trapping efficiency and the device compatibility for adherent single cell cultures. Before cell seeding, microfluidic devices were sterilized by autoclaving and dried overnight at 80°C. To favor cell adhesion on the glass substrate,

devices were air plasma treated for 5mins (Harrick Plasma) for increasing the hydrophilicity and subsequently overnight perfused with a 0.01% Poly-L-Lysine (PLL) solution (Sigma-Aldrich, Milano, Italy) at a flow rate of 30 μ l/hr. After trypsinization, U87-MG cells were diluted to the concentration of 2x10⁵ cells/mL and a single cell suspension was obtained by means of a cell strainer (40 μ m, Falcon®). Cells were then contemporarily seeded within the six culture units by perfusing the cell suspension through the seeding channels at a constant flow rate of 0.2 μ L/min for 5 minutes. Phase contrast images were thus acquired by means of Leica DMIRD inverted microscope and the trapping efficacy was calculated as the percentage of chambers containing a single cell over the total number of chambers *per* unit. Subsequently, a continuous flow rate of 2 μ l/min *per* line was imposed and the microfluidic platform was incubated under standard culture conditions and periodically monitored for assessing cell adhesion and proliferation.

3. Results

3.1 Computational optimization of the chamber geometry for single cell trapping

The proposed 8 configurations were compared in term of trapping efficacy through finite element analysis. Flow rates entering into the chambers were thus evaluated in both open and occluded configurations and compared to the corresponding Q_{lim} (Fig. 5a). In detail, a chamber inflow higher than Q_{lim} indicated the possibility of cells to enter into the chamber, while inflow lower than Q_{lim} ensured the chamber bypass. For all the considered combinations of channels and traps, the flow rate entering the chamber in the open configuration resulted higher than Q_{lim} , thus indicating all configurations as compatible with the trapping of cells in the selected size range ($\Phi=10\text{-}16\mu\text{m}$). Regarding the occluded configuration, different results were obtained based on the diameter of the simulated trapped cells. In detail, for bigger cells ($\Phi=16\mu\text{m}$) the percentage of flow entering the occluded chamber was smaller than Q_{lim} for all combinations. For smaller cells ($\Phi=10\mu\text{m}$), the portion of entering flow resulted higher than Q_{lim} for the $15\mu\text{m}$ traps, suggesting inability to isolate single cell, while lower for the $10\mu\text{m}$ traps, ensuring single cell trapping. This result indicated a higher efficacy of layouts featuring the $10\mu\text{m}$ wide trap for trapping single cells over a broader range of dimensions. The selectivity of cell trapping in correlation with the channel width was finally evaluate considering trapped cells with a diameter of $10\mu\text{m}$. Comparing the SI obtained for different channel widths and $10\mu\text{m}$ trap, the $50\mu\text{m}$ wide channel maximized this value, yielding the highest probability to trap only one cell (Fig. 5b). The same index resulted negative for the layouts featuring $15\mu\text{m}$ wide traps, confirming lower selectivity of these configurations.

3.2 Single cell trapping and culturing within the microfluidic device

Two devices ($50\mu\text{m}$ wide channel combined with both 10 and $15\mu\text{m}$ traps) were selected based on computational results for

biological experimental validation. In detail, U87-MG (diameter $15.4\pm 2.5\mu\text{m}$) were seeded within the microfluidic platform and cultured for up to 2 days. The proposed trapping mechanism allowed achieving a trapping efficiency of about 40%, having the six independent culture units simultaneously filled of individual cells within few minutes, for both considered trap dimensions. Cell seeded within the device adhered to the PLL functionalized substrate within 4 hours from the seeding maintaining high viability for up to 3 days in culture (Fig. 6).

4. Discussion

Aiming at pursuing direct and deterministic control over cause-effect relationships guiding cell behavior (Lindström and Andersson-Svahn, 2011; Schmid et al., 2010), many attempts have been made to couple the ability of microfluidics to handle single cells to defined spatial configuration and to precisely tailor the microenvironment around them (Lawrenz et al., 2012; Titmarsh et al., 2013). However, the existing approaches for trapping single cells within microfluidic devices mainly require complex and expensive fabrication procedures (Hanke et al., 2012; Hong et al., 2012; Wheeler et al., 2003). Herein, a low cost and single-layer PDMS microfluidic device was developed for isolation and culture of individual adherent cells into defined spatial configurations. The designed high-throughput platform integrated (i) a single cell culture area and (ii) an upstream serial dilution generator for delivering both soluble factors and non-diffusive molecules under spatio-temporally controlled chemical patterns.

The functionality of the two units was assessed in terms of (i) cell trapping efficiency and (ii) soluble and non-diffusive molecules mixing. The proposed trapping mechanism allows achieving high trapping efficiency, having the six independent culture units simultaneously filled of individual cells (diameter $16\mu\text{m}$) within few minutes. Trapped cells were also demonstrated to stay viable up to 3 days in culture.

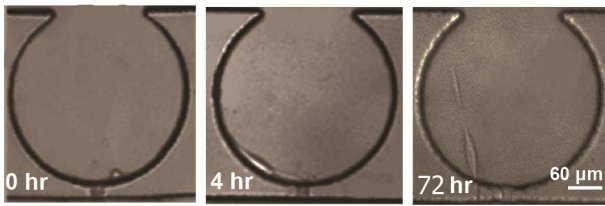


Fig. 6. The proposed mechanism allowed to trap single cells. Trapped cells started to adhere after 4hr from the seeding, maintaining high viability for up to 3 days in culture.

The generation of specific concentration patterns was then computationally optimized, exhibiting the potential to efficiently mixed both soluble factors and non-diffusive molecules (i.e. DNA vectors), generating defined concentration patterns to be delivered to cultured cells. The integration of this element allows extending the potential of the device for high-throughput screening over a wide range of molecules and particles.

5. Conclusions

The presented microfluidic platform represents a powerful tool for high-throughput screening at a single-cell level. Combining high trapping efficiency and ability to generate concentration patterns over a wide range of factors, the device will be useful for achieving more accurate control over input-output relationships guiding cell behavior.

Acknowledgements

This work was partially supported by Fondazione Cariplo, grant no. 2012-0891.

References

Andersson, H., van den Berg, A., 2003. Microfluidic devices for cellomics: a review. *Sensors and Actuators B-Chemical* 92, 315-325.

El-Ali, J., Sorger, P.K., Jensen, K.F., 2006. Cells on chips. *Nature* 442, 403-411.

Hanke, C., Waide, S., Kettler, R., Dittrich, P., 2012. Monitoring induced gene expression of single cells in a multilayer microchip.

Analytical and Bioanalytical Chemistry 402, 2577-2585.

Hong, S., Pan, Q., Lee, L.P., 2012. Single-cell level co-culture platform for intercellular communication. *Integrative Biology* 4, 374-380.

Jeon, N.L., Dertinger, S.K.W., Chiu, D.T., Choi, I.S., Stroock, A.D., Whitesides, G.M., 2000. Generation of solution and surface gradients using microfluidic systems. *Langmuir* 16, 8311-8316.

Lawrenz, A., Nason, F., Cooper-White, J.J., 2012. Geometrical effects in microfluidic-based microarrays for rapid, efficient single-cell capture of mammalian stem cells and plant cells. *Biomicrofluidics* 6.

Lindström, S., Andersson-Svahn, H., 2011. Miniaturization of biological assays — Overview on microwell devices for single-cell analyses. *Biochimica et Biophysica Acta (BBA) - General Subjects* 1810, 308-316.

Love, K.R., Bagh, S., Choi, J., Love, J.C., 2013. Microtools for single-cell analysis in biopharmaceutical development and manufacturing. *Trends in Biotechnology* 31, 280-286.

Mu, X., Zheng, W., Sun, J., Zhang, W., Jiang, X., 2013. Microfluidics for Manipulating Cells. *Small* 9, 9-21.

Schmid, A., Kortmann, H., Dittrich, P.S., Blank, L.M., 2010. Chemical and biological single cell analysis. *Current Opinion in Biotechnology* 21, 12-20.

Stroock, A.D., Dertinger, S.K.W., Ajdari, A., Mezić, I., Stone, H.A., Whitesides, G.M., 2002. Chaotic Mixer for Microchannels. *Science* 295, 647-651.

Titmarsh, D.M., Ovchinnikov, D.A., Wolvetang, E.J., Cooper-White, J.J., 2013. Full factorial screening of human embryonic stem cell maintenance with multiplexed microbioreactor arrays. *Biotechnology Journal* 8, 822-834.

Wang, H., 2012. *Angew. Chem., Int. Ed.* 51, 4349.

Wheeler, A.R., Thronset, W.R., Whelan, R.J., Leach, A.M., Zare, R.N., Liao, Y.H., Farrell, K., Manger, I.D., Daridon, A., 2003. Microfluidic device for single-cell analysis.

Analytical Chemistry 75, 3581-3586.

Xia, Y.N., Whitesides, G.M., 1998. Soft lithography. *Angew Chem Int Edit* 37, 551-575.